Highly Exfoliated Poly(ε-caprolactone)/ Organomontmorillonite Nanocomposites Prepared by *In Situ* Polymerization

Eylem Tarkin-Tas, Shailesh K. Goswami, Bishwa R. Nayak, Lon J. Mathias

Department of Polymer Science, University of Southern Mississippi, Hattiesburg, Mississippi 39406-0076

Received 19 February 2007; accepted 27 May 2007
DOI 10.1002/app.26964
Published online 28 September 2007 in Wiley InterScience (www.interscience.wiley.com).

ABSTRACT: Poly(ε-caprolactone)/organomodified montmorillonite nanocomposites were prepared by *in situ* polymerization with dibutyltin dimethoxide as an initiator/catalyst. The montmorillonite was first modified with 1-decyl-2-methyl-3-(11-hydroxyundecyl)imidazolium cation. The hydroxyl functionality was used not only for initiating polymer chains from the surface of the clay platelets but also for grafting polymer chains to the surface by acting as a reversible chain-transfer agent. The molecular weights of the polymer chains were controlled by the ratio of monomer to hydroxyl content. X-ray diffraction and transmission electron microscopy studies confirmed that highly exfoliated nanostructures were formed. The amount of inorganic component did not affect the thermal behavior of the polymer matrix as shown by differential scanning calorimetry or thermogravimetric analysis. The highly exfoliated clay sheets acted as nucleating agents and increased the degree of crystallinity from 51 to 69% at 5 wt %. Dynamic mechanical analysis revealed an enhancement of the storage modulus with increasing clay content above the glass-transition temperature. © 2007 Wiley Periodicals, Inc. J Appl Polym Sci 107: 976–984, 2008

Key words: biodegradable; mechanical properties; nanocomposites; organoclay; ring-opening polymerization

INTRODUCTION

In the field of high-performance materials, biodegradable polymer nanocomposites have been gaining interest because of their improved mechanical properties, barrier resistance, flame retardancy, solvent uptake, and rate of biodegradability compared to pristine polymers. The utility of layered silicate clays such as montmorillonite (MMT) to enhance polymer properties has been correlated to their high surface-area-to-volume ratio and their ability to interact with the polymer matrix.[1]

Clay sheets naturally occur in stacks. Thus, to become effective reinforcing agents, they must be well dispersed in the polymer matrix. Because of the hydrophilic nature of clay, its homogeneous dispersion in polymer matrices cannot be easily established. Clays modified with organic compounds are more organophilic and, thus, more compatible with polymer matrices. This is generally achieved by an ion-exchange reaction of the surface-bound inorganic cation with organic onium ions, such as phosphonium[2] or ammonium cations.[3] These oniums generally possess either long alkyl chains or chains bearing functional groups that are able to either interact with the polymer or initiate *in situ* polymerization.

The preparation of polymer nanocomposites is accomplished mainly by three processes. The most economical and straightforward method is the dry blending of components at predetermined compositions followed by melt mixing or extrusion.[4–6] Alternatively, the intercalation of polymer chains into the silicate layers can be accomplished from solvent dispersions or solutions.[7,8] The most efficient method, however, involves the intercalation of the monomer into the platelets followed by polymerization; this is also called *in situ polymerization.*[9] These methods can lead to either intercalated or exfoliated morphologies or a mixture of two or more nanostructures, depending on the preparation conditions and the level of interaction of the polymer matrix and clay. In intercalated structures, a few polymer chains are inserted between the clay layers without the destruction of their regularly alternating structure. In exfoliated structures, the stacks are delaminated, and individual clay sheets are dispersed randomly throughout the polymer matrix. In general, the exfoliation of the layers provides nanocomposites with better properties compared to intercalated structures, and such exfoliated morphologies are generally targeted.[1]

Poly(ε-caprolactone) (PCL) is a biodegradable aliphatic polyester that is synthesized by the ring-opening polymerization (ROP) of ε-caprolactone (ε-CL). It

Correspondence to: L. J. Mathias (lon.mathias@usm.edu).
Contract grant sponsor: Office of Naval Research.

can be degraded by microorganisms and undergoes facile hydrolysis. Its physical properties (a linear, flexible, and partially crystalline polyester) and commercial availability make it very attractive not only as a substitute for nondegradable polymers but also for application in medical devices, drug-delivery systems, and food packaging. Property limitations of PCL arise from its low melting temperature (T_m) and weak mechanical properties. The former can be overcome by blending with other polymers or by crosslinking. PCL-based nanocomposites offer the potential to improve its thermal stability, mechanical properties, barrier properties, and solvent resistance. Most attempts to date have used MMT because of its widespread availability, low cost, and environmental friendliness.[10]

Recently, the synthesis of PCL/MMT nanocomposites by both melt intercalation and *in situ* polymerization methods was reported by Dubois and coworkers.[11–18] PCL-based nanocomposites were prepared with different relative compositions of MMT, which was either natural or organomodified by various alkyl ammonium cations. The results showed that intercalated nanostructures were obtained by melt intercalation only when organically modified montmorillonite (OMMT) was used, whereas the *in situ* polymerization method gave better dispersion even with the unmodified natural clay. Other studies done by the same group have shown that the type of preparation method, the nature of the surfactant or organic modifier, and the content of organoclay all affected the morphological, mechanical, and thermal properties of the nanocomposites. *In situ* intercalative polymerization was found to be the most efficient method for obtaining near-to-exfoliated nanostructures and gave nanocomposites with much improved gas barrier, mechanical, and thermal properties. In general, such near-to-exfoliated morphology have been achieved when the natural clay was modified with hydroxyl groups containing alkyl ammonium cations, which can initiate the ROP of ε-CL. Hydroxyl groups can also be converted into metal alkoxides, which can be coactivators for polymerization and lead to grafted polyester chains.

The alkyl ammonium cations used for the preparation of polymer/organoclay nanocomposites generally exhibit poor thermal stability, especially in the preparation of nanocomposites by the melt intercalation method. Thermal degradation studies of alkyl-imidazolium salts and alkyl-imidazolium modified MMT have shown greater thermal stability compared to all alkyl–quaternary ammonium MMT.[19] Polystyrene,[20–22] polyamide 6, poly(ethylene terephthalate),[23] polypropylene,[24] and poly(ethylene naphthalate)[25] have been used to prepare nanocomposites with alkyl-imidazolium modified MMT by *in situ* polymerization, melt intercalation, and solvent blending methods. However, there has been no effort to use alkyl-imidazolium modified MMT with surfactant-bearing reactive functional groups for the synthesis of polyester-based nanocomposites. In addition, among the functionalized quaternary alkylammonium surfactants used to date, there have been no reports on the terminal functional groups on the long-alkyl chains attached to the surfactant.

In this study, MMT was treated with a novel alkyl-imidazolium surfactant bearing a terminal hydroxyl group on a long alkyl chain. The effects of the surfactant on polymer conversion and molecular weight, polymer grafting efficiency, and final nanocomposite properties were evaluated.

EXPERIMENTAL

Materials

ε-CL (99%) was purchased from Acros. Dibutyltin dimethoxide (Aldrich) was diluted with anhydrous toluene (Sigma-Aldrich). Sodium MMT with a cation exchange capacity of 93 mequiv/100 g was purchased from Southern Clay Products, Inc. 1-Decyl-2-methylimidazole and 11-bromo-1-undecanol were obtained from Aldrich and were used as received. PCL with two different molecular weights [PCL42500 number-average molecular weight (M_n) = 42,500 g/mol and PCL80000 M_n = 80,000 g/mol] was purchased from Aldrich. LiCl was dried in a vacuum oven before use (J. T. Baker Chemical Co.). THF, ethyl ether, and $CHCl_3$ were purchased from Fischer Scientific and were used without further purification.

Synthesis of 1-decyl-2-methyl-3-(11-hydroxyundecyl)imidazolium bromide (surfactant)

1-Decyl-2-methylimidazole (0.95 mol) was added to an excess of 11-bromo-1-undecanol (1 mol) in a thick-walled, single-necked, round-bottom flask equipped with a reflux condenser. The reaction mixture was heated to 100°C and allowed to react for 6 h under a nitrogen atmosphere. The white solid product was filtered and washed with ethyl acetate, and the solvent was removed *in vacuo* at 80°C. The isolated yield was 90%. The product was characterized by ^{1}H-NMR and ^{13}C-NMR spectroscopy.

^{1}H-NMR ($CDCl_3$, δ, ppm): 0.60 (t, CH_2—CH_3), 1.07 (m, 15xCH_2), 1.35 (m, N—CH_2—CH_2), 1.64 (m, CH_2—CH_2—OH), 2.63 (s, Ar—C—CH_3), 3.40 (t, CH_2—OH), 4.09 (t, N—CH_2), 7.46 (d, Ar—C*H*). ^{13}C-NMR ($CDCl_3$, δ, ppm): 10.8 (CH_2—CH_3); 13.9 (Ar—C—CH_3); 22.4, 25.5, 26.2, 29.3, 32.4 (15CH_2); 49.1 (2N—CH_2); 62.3 (CH_2—OH); 121.9 (Ar—*C*); 142.9 (Ar—*C*—CH_3).

Preparation of OMMT

The imidazolium salt (1.5 equiv of the CEC of MMT) was dissolved in ethanol at 50°C and added to a 10 wt % aqueous, predispersed suspension of MMT under vigorous stirring at 60°C. The mixture was stirred for 10 h at 60°C. The imidazolium-modified MMT (OMMT) was then collected by filtration, washed several times with hot deionized water and then with hot ethanol, and paper filtered. The hydroxyl alkyl-imidazolium modified MMT was dried at 80°C under vacuum for 24 h before use, and the organic content was determined by thermogravimetric analysis (TGA).

Preparation of the PCL/OMMT nanocomposites by the *in situ* intercalative polymerization of ε-CL

The typical polymerization procedure was as follows: The desired amounts of OMMT and ε-CL were added to a polymerization tube with the specified amount of monomer and dibutyltin dimethoxide. The reaction mixture was stirred at room temperature for 4 h under a nitrogen atmosphere. A solution of dimethyltin dimethoxide in anhydrous toluene was added. The temperature was increased to 100°C, and polymerization was allowed to proceed for 24 h. The crude product was dissolved in $CHCl_3$ and centrifuged for 15 min at 3300 rpm. The supernatant was removed and precipitated into ethyl ether. The white precipitate was filtered and dried in a vacuum oven at 40°C.

Nanocomposites containing 1, 2, 3, 4, and 5 wt % OMMT were prepared. The numbers in the abbreviations indicate the weight percentage of OMMT (i.e., PCL1 was the PCL/clay nanocomposite with 1 wt % hydroxyl alkyl-imidazolium modified MMT). The formation of PCL was determined by ^{1}H-NMR and ^{13}C-NMR in $CDCl_3$, solid-state ^{13}C-NMR, and Fourier transform infrared (FTIR) analysis.

^{1}H-NMR ($CDCl_3$, δ, ppm): 1.38 (m, γ-CH_2), 1.65 (m, β-CH_2 + δ-CH_2), 2.31 (t, α-CH_2), 3.65 (ε-CH_2—OH end group), 4.02 (t, ε-CH_2). ^{13}C-NMR ($CDCl_3$, δ, ppm): 24.6 (γ-CH_2), 25.6 (β-CH_2), 28.4 (δ-CH_2), 34.1 (α-CH_2), 64.2 (ε-CH_2), 173.4 (C=O). Solid-state ^{13}C-NMR (δ, ppm): 26.3 (γ-CH_2 + β-CH_2), 29.2 (δ-CH_2), 34.2 (α-CH_2), 64.5 (ε-CH_2), 174.3 (C=O). FTIR (λ^{-1}, cm^{-1}): 1727 (C=O).

Polymer recovery from the nanocomposites

The polymer chains were extracted from the clay by a reverse ion-exchange reaction. Thus, 1 g of the nanocomposite was suspended in 15 mL of THF and stirred for 2 h at room temperature. This solution was then poured into a 1 wt % LiCl solution in THF and stirred at room temperature for 48 h. The solution was centrifuged for 30 min, and the polymer-containing supernatant was collected. The solid fraction was washed twice with 15 mL of THF, and the supernatants were combined. The solvent was partially evaporated, and the polymer was precipitated into ethyl ether. The white powder was dried in a vacuum oven at 40°C.

Characterization of the nanocomposites

^{1}H-NMR and ^{13}C-NMR spectra were obtained in $CDCl_3$ with a Varian Mercury 300 spectrometer operating at 300 MHz for ^{1}H-NMR and 75 MHz for ^{13}C-NMR. Solid-state NMR spectroscopy was performed on a Varian UNITY INOVA 400 spectrometer with a standard Chemagnetics 7.5-mm PENCIL-style probe. Samples were loaded into zirconia rotor sleeves, sealed with Teflon caps, and spun at 4.0 kHz. The acquisition parameters were as follows: the ^{1}H 90° pulse width was 4.0 μs, the cross-polarization contact time was 1 ms, the dead time delay was 6.4 μs, and the acquisition time was 45 ms. A recycle delay of 3 s between scans was used. FTIR spectra were recorded on an ATI-Mattson Galaxy 5000 FTIR spectrometer.

Size exclusion chromatography (SEC) was carried out in THF (5 mg/mL) at 30°C with a Waters M-150-C ALC/GPC chromatograph equipped with a Viscotek differential viscometer (model 100) and styrene-DVB GPC columns (2 × Linear + 500, flow rate = 1 mL/min) and a Hewlett-Packard 1037A refractive-index detector. Molecular weights and molecular weight distributions were measured with respect to polystyrene standards.

Thermal analyses were performed on a TA Instruments SDT 2960 TGA–DTA at 10°C/min under nitrogen from ambient temperature to 700°C and a DSC 2920 at 10°C/min under nitrogen from −90 to 80°C. For differential scanning calorimetry (DSC) measurements, the samples were prepared with a melt press. They were melted at 85°C, held for 3 min at this temperature under about 3 MPa of pressure, and then quickly quenched between steel plates. All samples weighed in the range 6.0 ± 0.5 mg. The crystallization temperature (T_c), heat of crystallization, crystalline T_m, and heat of fusion (ΔH_f) were obtained by the following procedure. Samples were cooled to −90°C at a cooling rate of 10°C/min and held at this temperature for 2 min. Then, the temperature was increased to 80°C at a rate of 10°C/min and equilibrated at this temperature for 5 min to erase thermal history. The temperature was then decreased to −90°C and again increased to 80°C following the same procedure discussed previously.

X-ray powder diffraction (XRD) patterns were obtained using a Rigaku Ultima III X-ray diffractometer

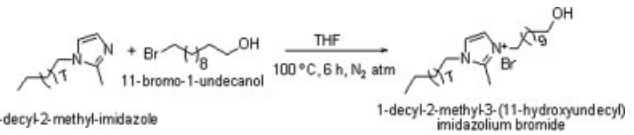

Figure 1 Synthesis of 1-decyl-2-methyl-3-(11-hydroxyundecyl)imidazolium bromide.

with Ni-filtered Cu Kα radiation (wavelength = 1.54 Å) and operated at 40 kV and 44 mA. XRD data were recorded between 2 and 45° at steps of 2°/min. Transmission electron microscopy (TEM) images of the samples were obtained using a Zeiss EM 10-C transmission electron microscope operating at an accelerating voltage of 50 kV. Ultrathin sections of the samples were taken with a microtome with a diamond knife and were collected on copper grids.

Thin films of samples were prepared with the same procedure used for DSC analysis. Dynamic mechanical analysis (DMA) of the samples was carried out under tension with a TA Instruments DMAQ800 at a heating rate of 2°C/min under nitrogen with a frequency of 1 Hz and a force of 0.1 N.

RESULTS AND DISCUSSION

Preparation of the nanocomposites

The synthesis of the surfactant is schematically illustrated in Figure 1. The product was isolated by filtration with excellent yield. The chemical structure of the surfactant was determined by its ^{1}H-NMR and ^{13}C-NMR spectra in $CDCl_3$.

The MMT was organically modified via an ion-exchange reaction between imidazolium and sodium cations with about 90% cation exchange efficiency. The organic content of OMMT was determined as 22 wt % by TGA. The onset decomposition temperature of bulk surfactant, 218°C, was increased to 285°C after incorporation onto MMT. The PCL nanocomposites with 1, 2, 3, 4, and 5 wt % OMMT content were prepared by *in situ* polymerization in bulk. Dibutyltin dimethoxide was used as an initiator/catalyst for coordination insertion polymerization, in which the ring opening of ε-CL involved the cleavage of the acyl–oxygen bond and the alkoxide groups form alkyl ester end groups.[26] The hydroxyl functionality of the surfactant served as a coinitiator/chain-transfer agent,[27] which used both grafting-from and grafting-to techniques. The amount of monomer and dibutyltin dimethoxide was kept constant for each polymerization vessel, whereas the hydroxyl content was increased by an increase in the OMMT content. The polymerization medium became highly viscous with increasing OMMT content. The crude products were dispersed in $CHCl_3$ and centrifuged to remove the nondispersed clay (not tethered to polymer chains). A small amount of precipitate was observed, but it could not be measured. This indicated that almost all polymer chains were grafted onto clay surfaces, and almost all clay surfaces had significant amounts of bound polymer.

The formation of the polymer was confirmed by ^{1}H-NMR and ^{13}C-NMR in $CDCl_3$, solid-state ^{13}C-NMR, and FTIR spectroscopy. The polymer chains were recovered via a reverse ion-exchange reaction, and molecular weights were determined by SEC. The theoretical molecular weights of PCL in the nanocomposites were calculated by the assumption that all hydroxyl groups of the surfactant on the clay and the alkoxide groups of dibutyltin dimethoxide were active. Table I shows that M_n decreased with increasing OMMT; this indicated that the PCL molecular weight was, in fact, controlled by the hydroxyl content of the bound surfactant. In addition, the narrow polydispersities (PDIs) were consistent with controlled initiation and polymerization.

To confirm that the hydroxyl functionality of the surfactant participated in the ROP of ε-CL, PCL with a low degree of polymerization was synthesized with the same surfactant under exactly the same conditions used for the preparation of the PCL/OMMT nanocomposites. Figure 2 shows the ^{1}H-NMR spectra of ε-CL, neat surfactant, and PCL synthesized with surfactant as the initiator (with a target degree of polymerization of 15). The disappearance of the peak at 3.40 ppm in spectrum B and the appearance of the peak at 4.22 ppm in spectrum C confirmed the conversion of the hydroxyl group of surfactant molecules to ester linkages upon reaction with ε-CL or PCL. In addition, the integrated area under the peak e was equal to the area under peak j, which was the alcohol end group of this low DP PCL. The degree of polymerization was determined from end-group analysis and found to be 12.

However, the characteristic ester peak seen in the low-molecular-weight PCL sample was not seen clearly in the ^{1}H-NMR spectra of the nanocomposites taken in $CDCl_3$. The reason might have been

TABLE I
Molecular Weight Determination

Sample	Conversion (%)	M_n (g/mol)[a]	M_n (g/mol)[b]	PDI[c]
PCL1	95	27,500	25,400	1.66
PCL2	93	23,300	24,700	1.60
PCL3	94	20,800	23,400	1.58
PCL4	87	17,200	19,800	1.60
PCL5	83	14,800	16,700	1.28

[a] $M_n = ([\varepsilon\text{-CL}]_0/2[\text{Sn}] + [\text{OH}]) \times M_{\varepsilon\text{-CL}} \times \text{Conversion (\%)}$.
[b] Determined by SEC.
[c] PDI = weight-average molecular weight/M_n.

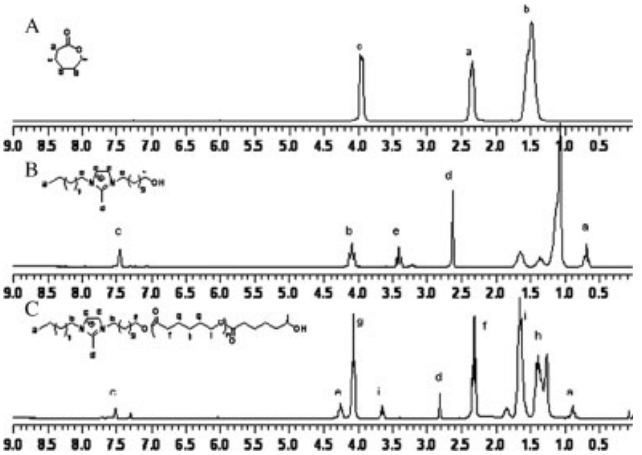

Figure 2 ^{1}H-NMR spectra of (A) ε-CL, (B) surfactant, and (C) PCL (DP = 12).

the presence of paramagnetic species in MMT (e.g., Fe^{3+}), which could have broadened the NMR peaks. In addition, the restricted mobility of the surfactant bonded to MMT could have made it difficult for us to observe bound peaks due to broadening. Fortunately, after the recovery of the polymer chain by ion exchange, the corresponding peak was observed in the ^{1}H-NMR spectrum at exactly the same value of 4.22 ppm (Fig. 3). However, due to the high molecular weight of the isolated PCL samples, the peak intensity was very low.

Morphological properties

XRD is one of the most commonly used technique for the initial characterization of nanocomposites. XRD patterns of the MMT, OMMT, PCL nanocomposites, and neat PCL are shown in Figure 4. The reflection at 2θ = 7.5°, with a corresponding *d*-spacing of 11.8 Å, was due to the stacked clay layers of

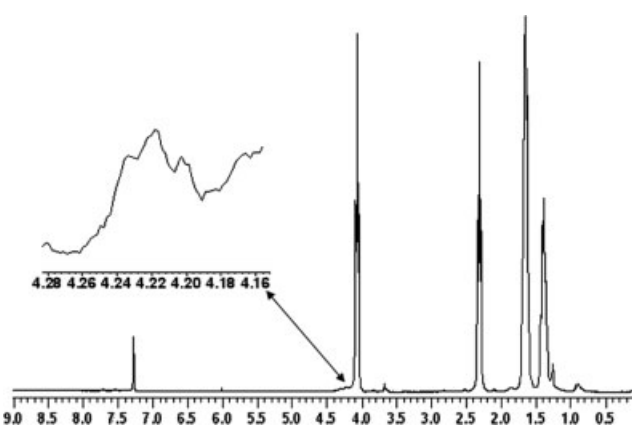

Figure 3 ^{1}H-NMR spectrum of recovered PCL from PCL5.

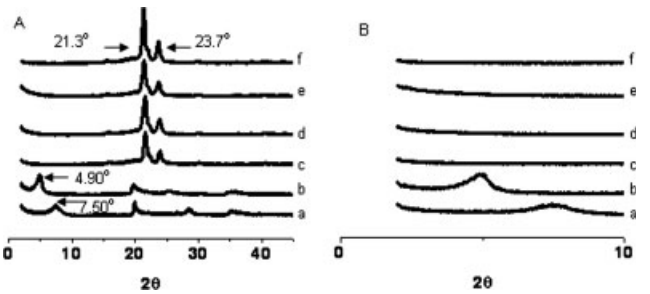

Figure 4 (A) XRD patterns of (a) MMT, (b) OMMT, (c) PCL1, (d) PCL3, (e) PCL5, and (f) neat PCL and (B) expanded XRD patterns between 0 and 10°.

MMT. When an intercalated nanostructure is obtained, the characteristic peak of stacked layers tends to shift to the lower angle region due to expansion of *d*-spacing. Thus, the *d*-spacing value was increased to 18.0 Å upon the modification of clay with surfactant, which indicated that the intercalation of the surfactant into the clay platelets took place without the destruction of the regular alternating stacking of the clay layers. In contrast, the complete disappearance of the peak was observed in the XRD patterns of the PCL nanocomposites due to loss of structural organization of the silicate layers. The two sharp reflection peaks at 2θ = 21.3 and 23.7° (corresponding to the crystalline structure of PCL) also appeared in the diffraction patterns of the PCL nanocomposites around the same 2θ values in all of the samples. Although the disappearance of the reflection peak corresponding to stacked platelets indicated a disordered structure, this did not provide information about whether the clay platelets were fully exfoliated and evenly dispersed throughout the polymer matrix. On the other hand, TEM analysis allowed direct visualization of the morphology, spatial distribution, and dispersion of the nanoparticles and platelets within the polymer matrix

TEM images from two different regions of a melt-pressed film of the PCL nanocomposite with 5 wt % OMMT content are shown in Figure 5. It is well known that the morphology of nanostructures is highly dependent on the interaction of the surfactant with the polymer matrix and the method of preparation of the nanocomposites. Previous studies have shown that near-to-exfoliated nanostructures can be achieved with alkyl–quaternary ammonium surfactants bearing hydroxyl ethyl or propyl groups for the *in situ* intercalative polymerization of ε-CL.[15–17] However, the hydroxyl functionality of these quaternary alkyl ammonium surfactants are on short alkyl chains close to the clay surface. In this study, the surfactant contained the hydroxyl functionality at the end of a long flexible alkyl chain, which may have provided better availability of the functional group for the initiation of the ROP of ε-CL. In other

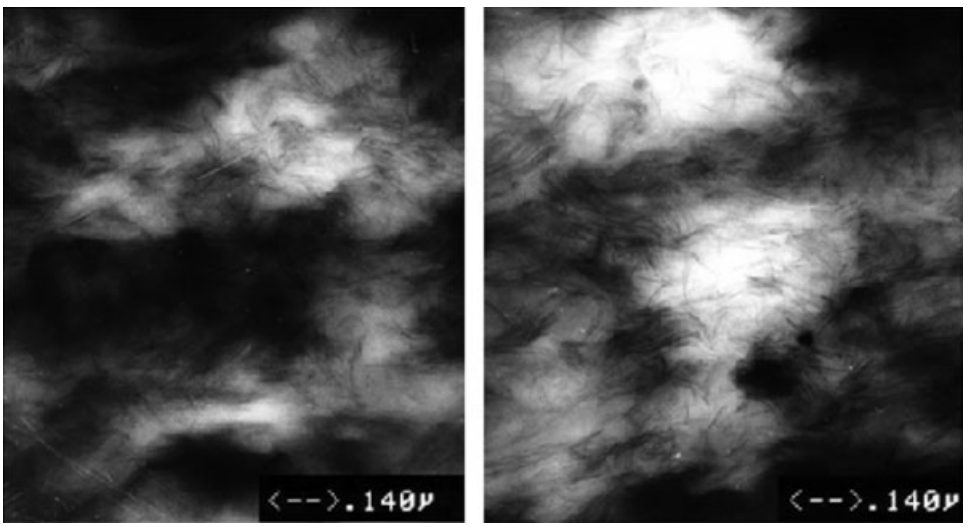

Figure 5 TEM images of PCL5 from two different regions.

words, the mobility of the terminal hydroxyl group on the long alkyl chain was not restricted by the clay surface, which in turn, may have allowed the monomer or nonbonded PCL chains to easily react with it. This could have increased the grafting efficiency of the polymer from the surface and led to a higher incorporation of polymer chains onto the clay platelets, which in turn, could have led to better exfoliation. The highly exfoliated morphology of the nanocomposites can be readily seen in Figure 5, where the individual clay platelets are exfoliated and distributed throughout the polymer matrix.

Thermal properties

The onset of thermal degradation temperatures (T_d's at 2 wt % loss) of these PCL/OMMT nanocomposites and commercial PCL were determined by TGA. The T_d values of the nanocomposites were very close to each other, and no trend with increasing clay content was observed. An increase in T_d with increasing clay content has been generally observed for intercalated nanocomposites.[8,28,29] The reason may be related to the loss of thermal mobility and the heat-transfer ability of chains confined between the platelets. In this case, the clay did not show any effect on degradation temperature due to its highly exfoliated nanostructure, which did not restrict thermal behavior or molecular mobility. Finally, the residual weights above 400°C were in accordance with the clay content.

The thermal properties of the nanocomposites and commercial PCL were further investigated by DSC. Both melting and crystallization processes of PCL

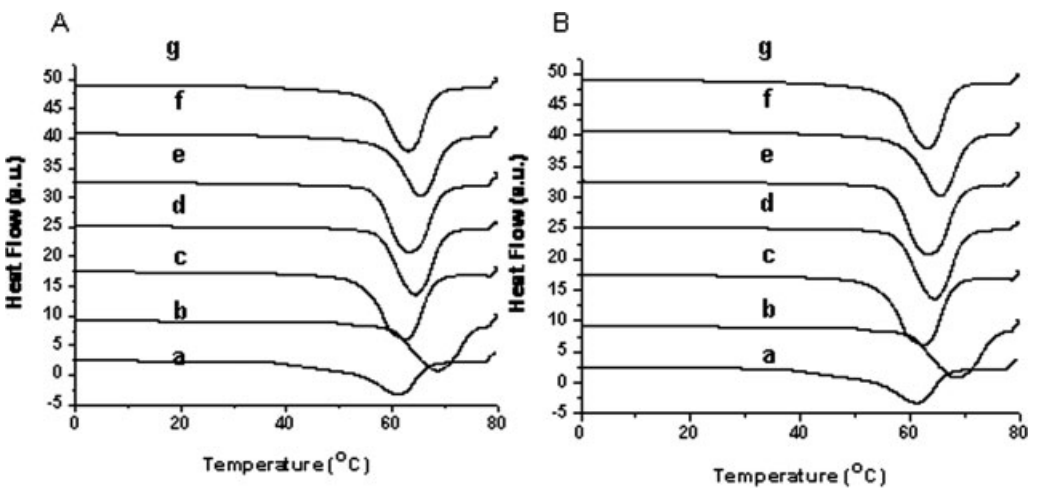

Figure 6 (A) Heating thermograms (Exo Up) of (a) PCL42500, (b) PCL80000, (c) PCL1, (d) PCL2, (e) PCL3, (f) PCL4, and (g) PCL5 and (B) cooling thermograms (Exo Up) of (a) PCL42500, (b) PCL80000, (c) PCL1, (d) PCL2, (e) PCL3, (f) PCL4, and (g) PCL5.

TABLE II
Thermal Properties of the PCL/OMMT Nanocomposites

Sample	T_m (°C)	ΔH_f (J/g)	T_c (°C)	ΔH_f (J/g)	Crystallinity (%)	T_d (°C)
PCL42500	58	69.9	18	65.1	51.3	342
PCL80000	61	74.3	19	69.0	54.6	363
PCL1	61	82.9	31	77.6	61.6	227
PCL2	62	75.6	30	79.3	56.7	210
PCL3	63	79.2	30	72.8	60.0	227
PCL4	62	82.4	30	75.5	63.1	219
PCL5	63	89.5	32	82.7	69.3	227

were detected in the heating and cooling thermograms (Fig. 6) of the nanocomposites, which indicated that the crystallization of the polymer chains was not inhibited by the inorganic component. In fact, the incorporation of even 1 wt % clay resulted in an obvious increase in T_c of PCL, indicating that the nanolayers were able to nucleate PCL crystallization.

The TGA and DSC results are summarized in Table II. The degree of crystallinity was calculated with ΔH_f for 100% crystalline PCL and was equal to 136 J/g[30] and normalized by W_{PCL}, which is the weight percentage of PCL in each nanocomposite {i.e., for PCL1, the degree of crystallinity = $[\Delta H_{f,exp}/(W_{PCL1} \times \Delta H_{f,th})] \times 100$, where W_{PCL1} = 0.99}. The results showed that both T_m and T_c were affected by increasing clay content. In addition, an increase in degree of crystallinity was observed with increasing clay content. Previous studies have shown that the degree of crystallinity is highly dependent on the morphology of the nanocomposites. For example, the absence of melting and crystallization transitions was observed by DSC measurements for PEO/MMT nanocomposites in which all polymer chains were intercalated. The bulk crystallization was effectively prohibited due to the confinement of the polymer chains between the layers.[31] In other studies, even though the conventional melting and crystallization curves of nanocomposites were obtained for intercalated nanocomposites as observed by DSC, the degree of crystallinity was either not affected by clay content or decreased with increasing clay content.[13,32–34] The thermal properties of PCL/OMMT nanocomposites were specifically investigated by Pucciarieollo et al.[35] Their results showed that the presence of an organophilic clay increased the degree of crystallinity of PCL when the nanocomposites were exfoliated but reduced the degree of crystallinity when the nanocomposites were intercalated. In this study, highly exfoliated silicate layers throughout the PCL matrix increased the surface area but with virtually all chains bound to the surfaces. This led to a preorganization of the chains near the platelets that enhanced nucleation and increased the degree of crystallinity with increasing clay content.

Mechanical properties

The morphology of polymer nanocomposites has a large influence on their mechanical properties. In general, exfoliated nanostructures lead to improved mechanical properties. In addition, due to the reinforcing ability of crystalline domains, the mechanical properties also tend to increase with degree of crys-

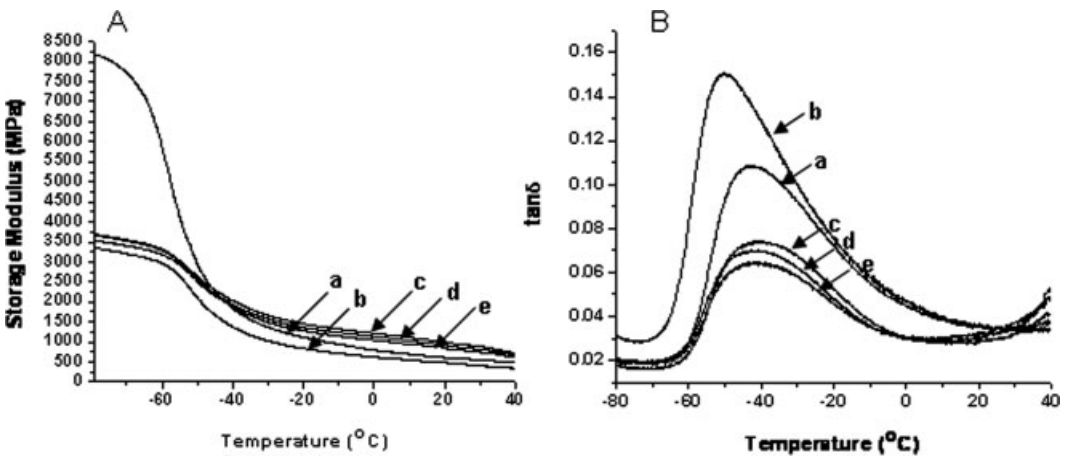

Figure 7 (A) Storage modulus versus temperature for (a) PCL80000, (b) PCL42500, (c) PCL1, (d) PCL2, and (e) PCL3 and (B) tan δ versus temperature for (a) PCL80000, (b) PCL42500, (c) PCL1, (d) PCL2, and (e) PCL3.

TABLE III
DMA Results

Sample	Storage modulus (MPa)			T_g (°C)
	−80°C	0°C	30°C	
PCL42500	3361	624	405	−42.4
PCL80000	7630	810	566	−50.6
PCL1	3551	1039	739	−42.3
PCL2	3710	1211	882	−42.7
PCL3	3842	1369	1001	−41.9

tallinity. Figure 7 shows representative storage modulus and tan δ curves as a function of temperature in the temperature range of −80 to +40°C. DMA of PCL4 and PCL5 was not performed because their films were brittle due to lower molecular weights of the PCL formed in these samples.

The average values of three measurements of storage modulus at −80, 0, and 30°C are listed in Table III. For all nanocomposites below the glass-transition temperature (T_g), the increase in storage modulus compared to neat commercial PCL42500 was not very high. Above T_g, however, the storage moduli of the nanocomposites were significantly higher than that of PCL. Specifically, they were higher by 70, 90, and 120% for PCL1, PCL2, and PCL3 at 0°C. At 30°C, the increase was greater at 80, 120, and 150% for PCL1, PCL2, and PCL3. When compared to PCL80000, the storage moduli of the nanocomposites were much lower at temperatures below T_g. However, above the T_g, again, there was a significant improvement in the storage modulus for the nanocomposites. This indicated that the reinforcing ability of the silicate layers was more significant in the rubbery rather than the glassy state.

The T_g values of the nanocomposites were not affected by the clay content and were essentially the same as that of the lower molecular weight commercial PCL. When the weight percentage clay content in the nanocomposites was converted to volume percentage (i.e., 1 wt % ≅ 0.5 vol %[6]), an effect of clay content on T_g was not expected. However, this also indicated that no confinement of polymer chains occurred, which could restrict the segmental mobility of polymer chains.

CONCLUSIONS

The molecular weight of PCL chains made by *in situ* polymerization was controlled by the terminal hydroxyl content; that is, by the OMMT content. The hydroxyl functionality on long alkyl chains had improved ability for the grafting of polymer chains from the surface of the clay, as verified by the highly exfoliated morphology obtained. Although this nanostructure did not markedly affect thermal events such as T_m, T_c, T_g, and T_d, the platelets clearly acted as nucleating agents for the crystallization of the PCL matrix, and the degree of crystallinity increased with clay content. DMA revealed the enhancement of storage moduli, particularly above T_g, with increasing the clay content. These results, plus the lack of precipitate formation from centrifuged $CHCl_3$ solutions, were consistent with the polymer chain ends being all (or mostly) bound to the clay surfactants.

References

1. Mai, Y. W.; Yu, Z. Z. Polymer Nanocomposites; Woodhead and CRC: Boca Raton, FL, 2006.
2. Imal, Y.; Inukai, Y.; Tateyama, H. Polym J 2003, 35, 230.
3. Usiki, A.; Kawasumi, M.; Kojima, Y.; Okada, A.; Karauchi, T.; Kamigaito, O. J Mater Res 1993, 8, 1174.
4. Ray, S. S.; Maiti, P.; Okamoto, M.; Yamada, K.; Ueda, K. Macromolecules 2002, 35, 3104.
5. Nam, J. Y.; Ray, S. S.; Okamoto, M. Macromolecules 2003, 36, 7126.
6. Chen, B.; Evans, J. R. G. Macromolecules 2006, 39, 747.
7. Aranda, P.; Hitzky, E. R. Chem Mater 1992, 4, 1395.
8. Lim, S. T.; Hyun, Y. H.; Choi, H. J.; Jhon, M. S. Chem Mater 2002, 14, 1839.
9. Kojima, Y.; Usuki, A.; Kawasami, M.; Okada, A.; Fukushima, Y.; Kurauchi, T.; Kamigaito, O. J Mater Res 1993, 8, 1185.
10. Pandey, J. K.; Reddy, K. R.; Kumar, A. P.; Singh, R. P. Polym Degrad Stab 2005, 88, 2, 234.
11. Viville, P.; Lazzoroni, R.; Pollet, E.; Alexandre, M.; Dubois, P.; Borcia, G.; Pireaux, J. J. Langmuir 2003, 19, 9425.
12. Gorrasi, G.; Tortora, M.; Vittoria, V.; Pollet, E.; Lepoittevin, B.; Alexandre, M.; Dubois, P. Polymer 2003, 44, 2271.
13. Gain, O.; Espuche, E.; Pollet, E.; Alexandre, M.; Dubois, P. J Polym Sci Part B: Polym Phys 2005, 43, 205.
14. Gorrasi, G.; Tortora, M.; Vittoria, V.; Pollet, E.; Lepoittevin, B.; Alexandre, M.; Dubois, P. J Polym Sci Part B: Polym Phys 2004, 42, 1466.
15. Lepoittevin, L.; Pantoustier, N.; Devalckenaere, M.; Alexandre, M.; Kubies, D.; Calberg, C.; Jerome, R.; Dubois, P. Macromolecules 2002, 35, 8385.
16. Kubies, D.; Pantoustier, N.; Dubois, P.; Rulmont, A.; Jerome, R. Macromolecules 2002, 35, 3318.
17. Lepoittevin, L.; Pantoustier, N.; Alexandre, M.; Calberg, C.; Jerome, R.; Dubois, P. Macromol Symp 2002, 183, 95.
18. Polet, E.; Delcourt, C.; Alexandre, M.; Dubois, P. Macromol Chem Phys 2004, 205, 2235.
19. Awad, W. H.; Gilman, J. W.; Nyden, M.; Haris, R. H.; Sutto, T. E., Jr.; Callahan, J.; Truvole, P. C.; DeLong, H. C.; Fox, D. M. Thermochim Acta 2004, 409, 3.
20. Gilman, J. W.; Awad, W. H.; Davis, R. D.; Shields, J.; Haris, R. H.; Davis, C., Jr.; Morgan, A. B.; Sutto, T. E.; Callahan, J.; Truvole, P. C.; DeLong, H. C. Chem Mater 2002, 14, 3776.
21. Bottino, F. A.; Fabbri, E.; Fragala, I. L.; Malandrino, M.; Orestano, A.; Pilati, F.; Pollicino, A. Macromol Rapid Commun 2003, 24, 1079.
22. Morgan, A. B.; Harris, J. D. Polymer 2004, 45, 8695.
23. Davis, C. H.; Mathias, L. J.; Gilman, J. W.; Schiraldi, D. A.; Shields, J. R.; Truvole, P.; Sutto, T. E.; Delong, H. C. J Polym Sci Part B: Polym Phys 2002, 40, 2661.
24. He, A.; Hu, H.; Huang, Y.; Dong, J. Y.; Han, C. C. Macromol Rapid Commun 2004, 25, 2008.
25. Chua, Y. C.; Lu, X.; Wan, T. J Polym Sci Part B: Polym Phys 2006, 44, 1040.
26. Krichheldrof, H. R.; Berl, M.; Scharnagl, N. Macromolecules 1988, 21, 286.

27. Penczek, S.; Biela, T.; Duda, A. Macromol Rapid Commun 2000, 21, 941.
28. Lepoittevin, B.; Devalckenaere, M.; Pantoustier, N.; Alexandre, M.; Kubies, D.; Calberg, C.; Jerome, R.; Dubois, P. Polymer 2002, 43, 4017.
29. Lepoittevin, B.; Pantoustier, N.; Devalckenaere, M.; Alexandre, M.; Calberg, C.; Jerome, R.; Henrist, C.; Rulmont, A.; Dubois, P. Polymer 2003, 44, 2033.
30. Crescenzi, V.; Manzini, G.; Calzolari, G.; Borri, C. Eur Polym J 1972, 8, 449.
31. Vaiva, R. A.; Sauer, B. B.; Tse, O. K.; Giannelis, E. P. J Polym Sci Part B: Polym Phys 1997, 35, 59.
32. Di, Y.; Iannace, S.; Maio, E. D.; Luigi Nicolais, L. J Polym Sci Part B: Polym Phys 2003, 41, 670.
33. Jimenez, G.; Ogata, N.; Kawai, H.; Ogihara, T. J Polym Sci Part B: Polym Phys 1997, 64, 2211.
34. Tortora, M.; Vittoria, V.; Galli, G.; Ritrovati, S.; Chiellini, E. Macromol Mater Eng 2002, 287, 243.
35. Pucciarieollo, R.; Villani, V.; Belviso, S.; Gorrasi, G.; Tortora, M.; Vittoria, V. J Polym Sci Part B: Polym Phys 2004, 42, 1321.